AIMS Mathematics

http://www.aimspress.com/journal/Math

AIMS Mathematics, 7(3): 3972–3987.
DOI: 10.3934/math.2022219
Received: 08 October 2021
Accepted: 17 November 2021
Published: 13 December 2021

Research article

3D-Chaotic discrete system of vector borne diseases using environment factor with deep analysis

Shaymaa H. Salih[1] **and Nadia M. G. Al-Saidi**[2,*]

[1] Department of Mathematics, College of Science, Mustansiriyah University, Iraq
[2] Department of Applied Sciences, University of Technology, Iraq

* **Correspondence:** Email: nadia.m.ghanim@uotechnology.edu.iq.

Abstract: Vector-Borne Disease (VBD) is a disease that consequences as of an infection communicated to humans and other animals by blood-feeding anthropoids, like mosquitoes, fleas, and ticks. Instances of VBDs include Dengue infection, Lyme infection, West Nile virus, and malaria. In this effort, we formulate a parametric discrete-time chaotic system that involves an environmental factor causing VBD. Our suggestion is to study how the inclusion of the parasitic transmission media (PTM) in the system would impact the analysis results. We consider a chaotic formula of the PTM impact, separating two types of functions, the host and the parasite. The considered applications are typically characterized by chaotic dynamics, and thus chaotic systems are suitable for their modeling, with corresponding model parameters, that depend on control measures. Dynamical performances of the suggested system and its global stability are considered.

Keywords: differential operator; fractal chaotic system; fractal; locally fractional calculus; fractal dynamic system; difference system
Mathematics Subject Classification: 37M20, 34H10

1. Introduction

The mathematical modeling system of VBD (discreet formula as well as the continuous type) is presented by many researchers depending on the developments of VBD [1]. Dye [2] suggested the simple population system by the formula

$$P(\top + \tau) = \frac{\rho P(\tau)}{(1 + \varrho P(\tau))^{\gamma}}, \tag{1}$$

where $P(\tau), P(\top + \tau)$ indicate the population magnitudes in straight groups, and ρ is the finite rate of growth (net fertility after lifetime density autonomous humanities). For ϱ is water containers, and

γ is the upper slope of the association between humanity and log population magnitude. May [3] formulated the following model

$$P(\top + \tau) = (\rho P(\tau)) \exp(-\varrho\, P(\tau)). \tag{2}$$

Then Bellows [4] presented the design

$$P(\top + \tau) = (\rho P(\tau)) \exp(-\varrho\, P^{\gamma}(\tau)). \tag{3}$$

Recently, systems (1)–(3) are generalized into 2D-systems called the parasitoid-host system (PHS) [5]

$$\begin{aligned} H(\top + \tau) &= (\rho_1 H(\tau))\,(F(P(\tau), H(\tau))) \\ P(\top + \tau) &= (\rho_2 H(\tau))\,(1 - F(P(\tau), H(\tau))) \end{aligned} \tag{4}$$

where

- H, P are the population densities for host and parasitoid accordingly;
- $F : \mathbb{R}_+ \times \mathbb{R}_+ \to \mathbb{R}_+$ takes one of the formulas in (1)–(3) and it indicates the fraction of host population that does not para-sized (infected). Special forms are given as follows: $F(P(\tau), H(\tau)) = \exp(-\varrho\, P^{\gamma})$ and $F(P(\tau), H(\tau)) = (1 + \varrho P(\tau))^{-\gamma}$. Note that when $\gamma = 1$, we have the logistic function $F(P(\tau), H(\tau)) = (1 + \varrho P(\tau))^{-1}$. Moreover, it can be formulated by $F(P(\tau), H(\tau)) = \exp(-\varrho\, P^{\tau})$ (see [5]). In our study, we suggest the Hyperbolic tangent, which is the shifted and scaled type of the logistic function $F(P(\tau), H(\tau)) = \tanh(P(\tau))$. This function is listed as an activation function as well as a Sigmoid function (utility function). As an application, it can be utilized in the field of artificial intelligence, especially the artificial neural network [6, 7].
- ρ_1 represents the size of the growth of the host;
- ρ_2 is the rate of a parasitoid population;
- $\tau, \top$ is the recent time and its iteration respectively.

Different studies are considered for system (4) by researchers and investigators. Din [8] adapted the PHS with the application of constant retreat effects and described global dynamics for the projected model. In [9], the authors reformed the PHS with a growth function for the host population and considered Neimark-Sacker bifurcation and chaos control. In [10], global stability and Hopf bifurcation approved a class of PHS.

We proceed to define the third dimension of our system. We suggest including an environment factor called parasitic transmission media (PTM), which includes all types of garbage, water, food, and air. Human health is at hazard through our indecision. We keep creating large amounts of garbage, we do not place of it properly, and in the end that will be our breakdown as it is for the environment and nature in the bionetworks we all stake. We cannot avoid or promote longevity with how we delight our Earth. The more emissions that we create due to how much trash we produce, affects us long term. One can progress diseases such as asthma, birth defects, cancer, cardiovascular disease, childhood cancer, COPD, infectious diseases, low birth weight, and preterm delivery. Bacteria, vermin and insects can also be recognized to the problem that garbage effects.

The dynamic variable $G(\tau)$ defines the mass of PTM in a specific PTM grip at time τ where $0 \leq \tau \leq 24$ and $\top \in \mathbb{R}$. As the system profits day-to-day garbage gathering, the time scale of deliberation will be 24 hours and the unit of time utilized will be "hours". The mass of PTM $G(\tau)$ will be sized

depending on its type. It is presumed that between time τ and $\top + \tau$, a total of $H(\tau)$ number of persons credit the PTM in the grip. The number of active garbage removal units at time τ is given by $P(\tau)$, the amount of PTM left in the hold under the effect of these two functions is given by the chaotic equation [11]

$$G(\top + \tau) = G(\tau) + \alpha_1 H(\tau) - \alpha_2 P(\tau), \tag{5}$$

where α_1 is the mass of PTM given per person per unit time, α_2 is the mass of PTM removed by removal unit per unit time. Here, we define the chaotic formula of (5) as follows:

$$G(\top + \tau) = \alpha_0 G(\tau) + \alpha H(\tau) + (1 - \alpha) P(\tau), \tag{6}$$

where $\alpha_0 > 0$ indicates the cumulative mass and $\alpha \in [0, 1]$. Combining 2D-System (4) and and Eq (6) to obtain the following 3D-discrete dynamic system

$$\begin{aligned} H(\top + \tau) &= (\rho_1 H(\tau))\,(F(P(\tau), H(\tau))) \\ P(\top + \tau) &= (\rho_2 H(\tau))\,(1 - F(P(\tau), H(\tau))) \\ G(\top + \tau) &= \alpha_0 G(\tau) + \alpha H(\tau) + (1 - \alpha) P(\tau). \end{aligned} \tag{7}$$

The remaining study in this paper is that the permanence of outcomes of Model (7) is reflected. Global stability investigations of the set of fixed points of Model (7) are considered. The control strategy is established for controlling the chaotic and fluctuating condition of Model (7) about its fixed points. In the end, numerical simulations are given to confirm the mathematical investigations.

2. Illustrated systems

In this part, we illustrate a set of systems that are relevant to System (7). In the sequel, we deal with the following structure.

$$\begin{aligned} H_{n+1} &= (\rho_1 H_n)\,(F(P_n, H_n)) \\ P_{n+1} &= (\rho_2 H_n)\,(1 - F(P_n, H_n)) \\ G_{n+1} &= \alpha_0 G_n + \alpha H_n + (1 - \alpha) P_n. \end{aligned} \tag{8}$$

For special case, we assume that $F(P_n, H_n) = \tanh(P_n)$, (see Figure 1) we have the following system

$$\begin{aligned} H_{n+1} &= (\rho_1 H_n)\,(\tanh(P_n)) \\ P_{n+1} &= (\rho_2 H_n)\,(1 - \tanh(P_n)) \\ G_{n+1} &= \alpha_0 G_n + \alpha H_n + (1 - \alpha) P_n. \end{aligned} \tag{9}$$

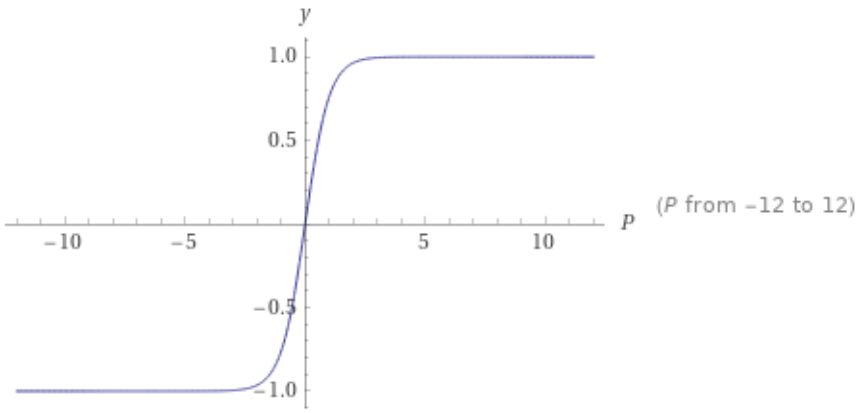

Figure 1. The plot of tanh(P).

We note that tanh(.) is an activation function that income, we can catch the slope of the sigmoid arc at every two points. Production values are bound between zero and one (during the first epoch of training), normalizing the output of every point. Also, the activation function tanh has a symmetric value [-1,1]; henceforth, it types the strata lying to quicker saturation.

Moreover, one can generalize Model (9), by using the difference operator

$$\eth(X_n) := X_{n+1} - X_n$$

to formulate the model

$$\begin{aligned} H_{n+1} - H_n &= (\rho_1 H_n)\,(\tanh(P_n)) - H_n \\ P_{n+1} - P_n &= (\rho_2 H_n)\,(1 - \tanh(P_n)) - P_n \\ G_{n+1} - G_n &= \alpha_0 G_n + \alpha H_n + (1-\alpha)P_n - G_n. \end{aligned} \tag{10}$$

This implies the model

$$\begin{aligned} \eth(H_n) &= (\rho_1 H_n)\,(\tanh(P_n)) - H_n \\ \eth(P_n) &= (\rho_2 H_n)\,(1 - \tanh(P_n)) - P_n \\ \eth(G_n) &= \alpha H_n + (1-\alpha)P_n - (1-\alpha_0)G_n. \end{aligned} \tag{11}$$

Finally, the continuous model with respect to time t is formulated as follows:

$$\begin{aligned} \frac{d}{dt}H(t) &= (\rho_1 H(t))\,(\tanh(P(t))) - H(t) \\ \frac{d}{dt}P(t) &= (\rho_2 H(t))\,(1 - \tanh(P(t))) - P(t) \\ \frac{d}{dt}G(t) &= \alpha H(t) + (1-\alpha)P(t) - (1-\alpha_0)G(t). \end{aligned} \tag{12}$$

The Jacobian matrix of Model (11) is given by

$$\mathbf{J} = \begin{pmatrix} \frac{\partial f_1}{\partial H} & \frac{\partial f_1}{\partial P} & \frac{\partial f_1}{\partial G} \\ \frac{\partial f_2}{\partial H} & \frac{\partial f_2}{\partial P} & \frac{\partial f_2}{\partial G} \\ \frac{\partial f_3}{\partial H} & \frac{\partial f_3}{\partial P} & \frac{\partial f_3}{\partial G} \end{pmatrix} = \begin{pmatrix} \rho_1 \tanh(P) - 1 & \rho_1 H \operatorname{sech}^2(P) & 0 \\ \rho_2(1 - \tanh(P)) & -\rho_2 H \operatorname{sech}^2(P) - 1 & 0 \\ \alpha & \alpha - 1 & \alpha_0 - 1 \end{pmatrix}$$

where

$$\begin{pmatrix} f_1(H,P,G) \\ f_2(H,P,G) \\ f_3(H,P,G) \end{pmatrix} = \begin{pmatrix} (\rho_1 H)(\tanh(P)) - H \\ (\rho_2 H)(1 - \tanh(P)) - P \\ \alpha H - (1-\alpha)P - (1-\alpha_0)G \end{pmatrix}.$$

Thus, we have

$$\begin{aligned} |\mathbf{J}| &= (\alpha_0 - 1)\left(-(\rho_1 - 1)\rho_2 H \operatorname{sech}^2(P) - \rho_1 \tanh(P) + 1\right) \\ &\approx (\rho_1 - 1)(1 - \alpha_0), \quad P \to \infty. \end{aligned}$$

The set of eigenvalues of $\mathbf{J}$ is

$$\begin{aligned} \Lambda := \Big\{ & \lambda_1 = \alpha_0 - 1, \\ \lambda_{2,3} = & \frac{\pm 0.707 \sqrt{\rho_1^2[\cosh(4P) - 1] + 8\rho_1\rho_2 H[2\cosh(2P) + 2 - \sinh(2P)] + 8\rho_2^2 H^2}}{2(\cosh(2P) + 1)} \\ & + \frac{\rho_1 \sinh(2P) - 2\rho_2 H - 2\cosh(2P) - 2}{2(\cosh(2P) + 1)} \Big\} \end{aligned}$$

Model (11) has the following set of fixed points satisfying $H_{n+1} = H_n, P_{n+1} = P_n, G_{n+1} = G_n$

$$\begin{aligned} \Phi := & \Big\{ \varphi_0(0,0,0), \\ & \varphi_1\left(\frac{\rho_1 \log\left(\sqrt{\frac{\rho_1+1}{\rho_1-1}}\right)}{\rho_2(\rho_1 - 1)}, \log\left(\sqrt{\frac{\rho_1+1}{\rho_1-1}}\right), \frac{[\rho_2(\rho_1-1)(\alpha-1) - \alpha\rho_1]\log\left(\sqrt{\frac{\rho_1+1}{\rho_1-1}}\right)}{\rho_2(\rho_1-1)(\alpha_0-1)} \right) \Big\} \\ & := \left\{ \varphi_0(0,0,0), \varphi_1\left(\frac{\rho_1 \ell}{\rho_2(\rho_1-1)}, \ell, \frac{[\rho_2(\rho_1-1)(\alpha-1) - \alpha\rho_1]\ell}{\rho_2(\rho_1-1)(\alpha_0-1)} \right) \right\}, \end{aligned}$$

where $\ell := \log\left(\sqrt{\frac{\rho_1+1}{\rho_1-1}}\right)$ providing that $\rho_1 \neq 1$, $\alpha_0 \neq 1$ and $\rho_2 \neq 0$. Hence, for $\alpha_0 = 2$, we get the following cases of the set of the eigenvalues

- $$\Lambda_{\varphi_0} = \Big\{ \lambda_1 = 1, \lambda_{2,3} = -1 \Big\},$$

  which dominated an attracting saddle. This surface has an unstable eigenvalue generating one direction of outflow behavior and two stable eigenvalues generate a plane involving all the inflow streamlines (see Figures2–4);

- assuming $\alpha = 0$, we obtain $\varphi_1(\ell(\mathfrak{b}, 1, -1))$, where $\mathfrak{b} := \dfrac{\rho_1}{\rho_2(\rho_1 - 1)}$ then

$$\begin{aligned}\Lambda_{\varphi_1} = \Big\{&\lambda_1 = 1,\\ &\lambda_{2,3} = \pm 0.0071\ell\sqrt{(1 - 2e^4 + e^8)\rho_1^2 + 8e^2(3 + 4e^2 + e^4)\rho_1\rho_2\mathfrak{b} + 16e^4\rho_2^2\mathfrak{b}^2}\\ &+ \ell(0.381\rho_1 - 0.21\rho_2\mathfrak{b} - 1)\Big\}\end{aligned}$$

- when $\alpha = 1$, we have $\varphi_1(\ell(\mathfrak{b}, 1, \mathfrak{b}))$, which implies the same eigenvalues in Λ_{φ_1}, where $\alpha = 0$ and $\alpha = 1$ are the end points of the chaotic Model (11).
- If $\rho_1 = \rho_2 \neq 1$, then we have $\mathfrak{b} = 1/(1 - \rho_1)$ and

$$\begin{aligned}\Lambda_{\varphi_1} = \Big\{&\lambda_1 = 1,\\ &\lambda_{2,3} = \pm 0.0071\ell\rho_1\sqrt{850\mathfrak{b}^2 + 4974\mathfrak{b} + 2719} + \ell(0.38\rho_1 - 1 - 0.21\rho_1\mathfrak{b})\Big\}.\end{aligned}$$

  Note that the zeros of $\sqrt{850\mathfrak{b}^2 + 4974\mathfrak{b} + 2719}$ are $\mathfrak{b}_1 = -0.6$ and $\mathfrak{b}_2 = -5.24$. This leads to the approximated values of $\lambda_{2,3} \approx 0.00636$ and $\lambda_{2,3} \approx 1.0405$ respectively, when $\rho_1 = 2$. More approximation yields

$$\Lambda_{\varphi_1} = \Big\{\lambda_1 = 1, \lambda_{2,3} = 0.01\Big\}$$

  and

$$\Lambda_{\varphi_1} = \Big\{\lambda_{1,2,3} \approx 1\Big\}.$$

- The set of equilibrium points is as follows:

$$\Xi = \Big\{\psi_0(0,0,0), \psi_1(0, P, \frac{P(1-\alpha)}{\alpha_0}), \psi_2(H, -\frac{\alpha H}{\alpha - 1}, 0), \psi_3(H, P, \frac{P - \alpha(H+P)}{\alpha_0})\Big\}.$$

Consequently, we have

$$\mathbf{J}_{\psi_0} = \begin{pmatrix} -1 & 0 & 0 \\ \rho_2 & -1 & 0 \\ \alpha & \alpha - 1 & \alpha_0 - 1 \end{pmatrix}$$

with the following set of eigenvalues

$$\Lambda_{\psi_0} = \{\lambda_{1,2} = -1,\ \lambda_3 = \alpha_0 - 1\},$$

which is equal to the set Λ_{φ_0} when $\alpha_0 = 2$. Model (11) has a saddle surface (see Figures 2–4 for the generation of the point), which satisfies the max-min inequality

$$\sup_{u\in U}\inf_{v\in V}\sigma(u,v) \leq \inf_{v\in V}\sup_{u\in U}\sigma(u,v), \quad \sigma : U \times V \to \mathbb{R}.$$

Moreover, Model (9) is permanent if the inequality holds:

$$\mu_1 \leq \lim_{n\to\infty}\inf(H_n, P_n, G_n) \leq \lim_{n\to\infty}\sup(H_n, P_n, G_n) \leq \mu_2, \quad 0 < \mu_1 \leq \mu_2,$$

where $S = \{(H_N, P_n, G_n)\}$ is a positive solution for Model (9).

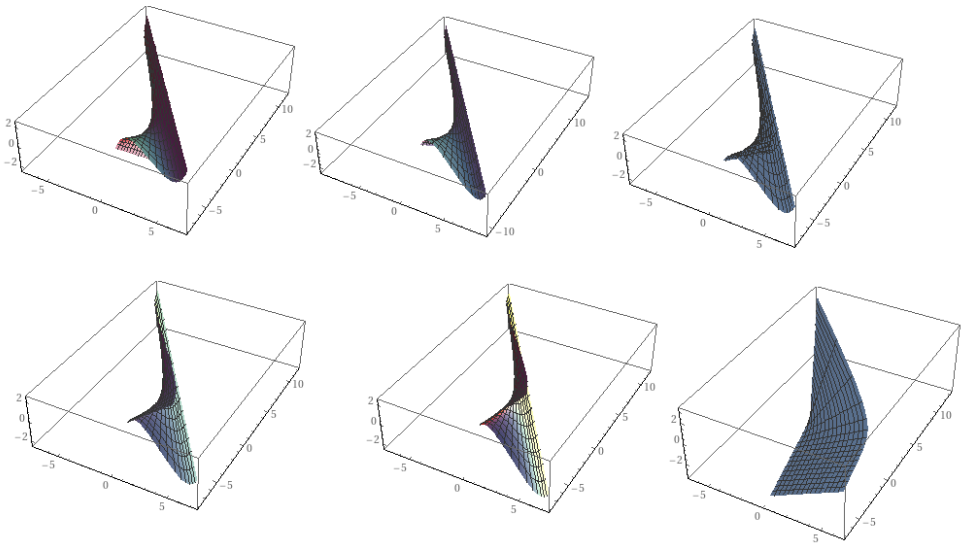

Figure 2. The 3D-plot of Model (11), when $\rho_1 = \rho_2 = 2$ for $\alpha = 0, 0.25, 0.5, 0.75, 1$ and the periodic solution (when $\alpha = 0.5$) respectively.

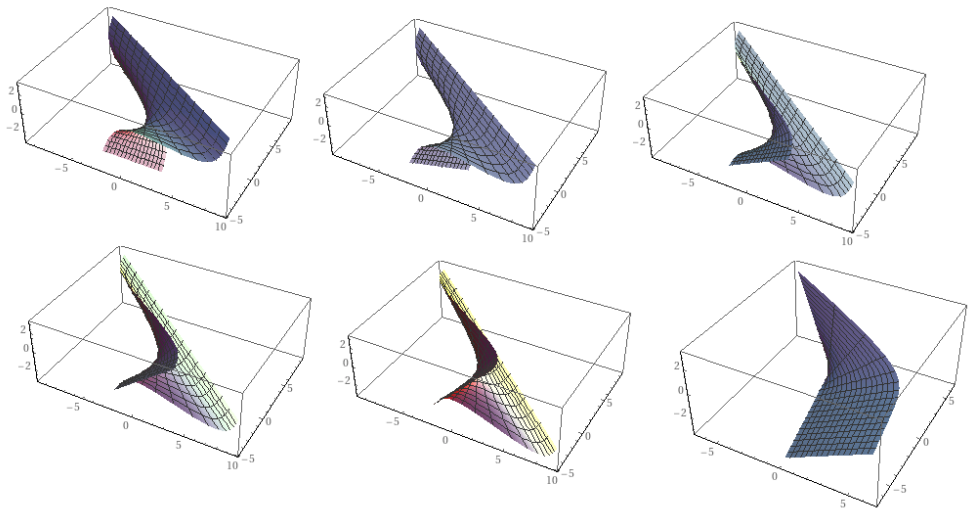

Figure 3. The 3D-plot of Model (11), when $\rho_1 = 2, \rho_2 = 1$ for $\alpha = 0, 0.25, 0.5, 0.75, 1$ and the periodic solution (when $\alpha = 0.5$) respectively.

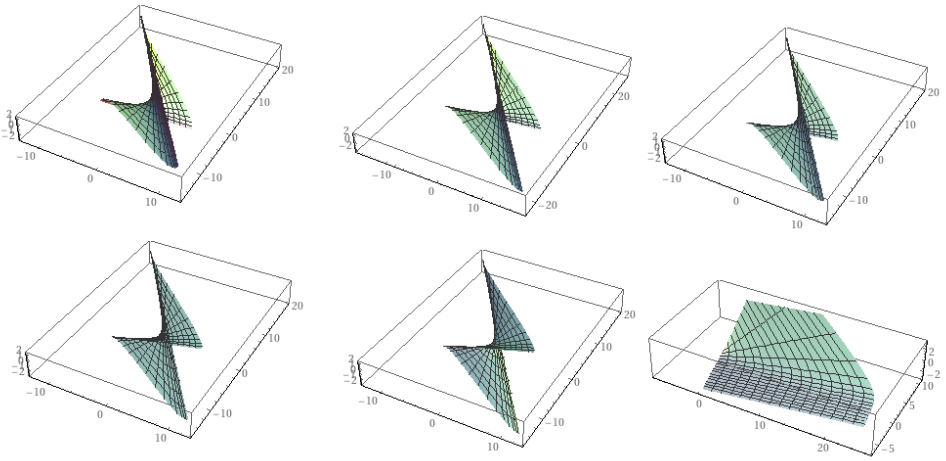

Figure 4. The 3D-plot of Model (11), when $\rho_1 = 5, \rho_2 = 4$ for $\alpha = 0, 0.25, 0.5, 0.75, 1$ and the periodic solution (when $\alpha = 0.5$) respectively. It is clear that the point (0,0,0) on the saddle corresponds to a degenerate critical point of the function $G(H, P)$ at (0, 0) providing that $|1 - \alpha_0| < \epsilon, \epsilon > 0$ is small enough.

Since complex behavior means that small changes to parameters or initial conditions can have large effect on the biological system in long term, therefore, the reconstruction of the system offers (chaotic system) an important tool to study the vector field and the biological dynamics.

3. Chaotic system

Chaos is a corporate factor that can exist in dynamical systems (discrete and continuous). Due to its properties, it has several applications (see [12–15]). Numerous indications represent that numerous biological models, particularly the human brain, perform in both chaotic and periodic styles. Researchers presented that the brain's utility permanently changes between various conditions. These interchanges are because of irregularity or illnesses. Given that a beneficial instrument for scrutinizing and improved considering of biological models, chaotic models have recurrently utilized in investigative studies to analyze and formulate biological models (see [16–18]). The result curves to chaotic systems commonly show fractal construction. The construction of the bizarre attractions for general n-dimensional systems might be convoluted and problematic to detect evidently. The subsequent appearances are approximately permanently showed by the resolutions of chaotic systems (see Figures 5–7):

- Long-term episodic (non- episodic) conduct: the difficulty to realize the difference between episodic and non- episodic conduct.
- Sympathy to initial conditions: depending on initial conditions.
- Fractal construction: the outcome plots to chaotic systems normally show a fractal structure

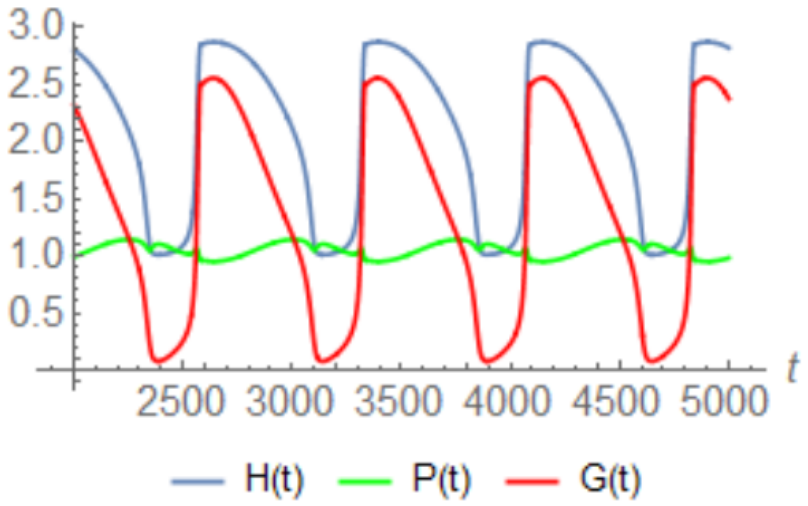

Figure 5. The conduct of the chaos, when $\rho_1 = 1.3, \rho_2 = 1.1, \alpha_0 = 0.45, \alpha = 0.34$. It is clear that PTM is controlled by the hosted population. Therefore, parasitoid decreases.

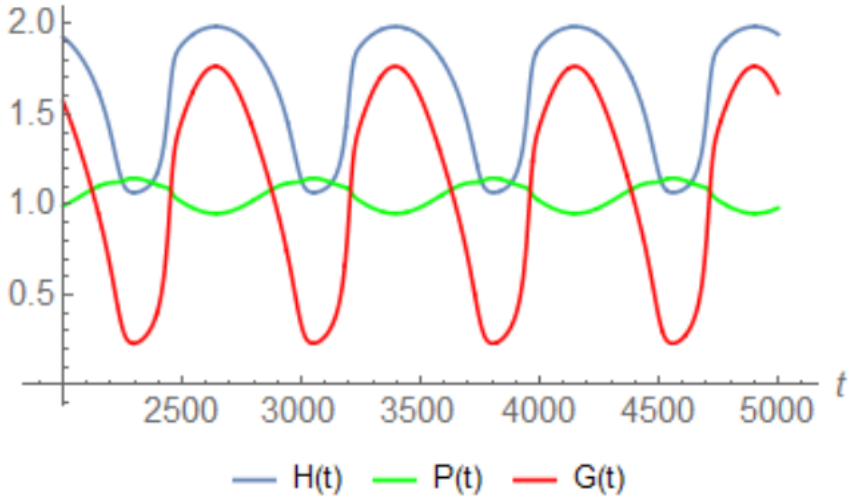

Figure 6. The conduct of the chaos, when $\rho_1 = \rho_2 = 1.1, \alpha_0 = 0.45, \alpha = 0.34$. It is clear that PTM is controlled by the hosted population. Therefore, parasitoid decreases.

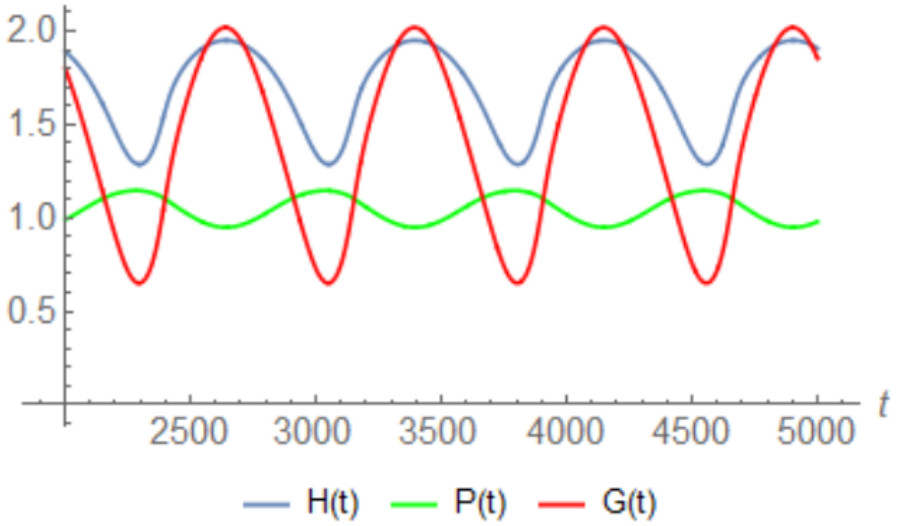

Figure 7. The conduct of the chaos, when $\rho_1 = 1.1, \rho_2 = 1.1, \alpha_0 = 0.6, \alpha = 0.4$. It is clear that PTM is not under control. Therefore, parasitoid increases.

Theorem 1. *Suppose that* $S = \{(H_n, P_n, G_n)\}$ *is a positive solution for Model* (9). *If* $\rho_1 > 1$, $\rho_2 \in (0, \rho_1]$ *and* $\alpha_0 \in (0, 1)$ *then Model* (9) *is permanent. Moreover, the model has a saddle surface.*

Proof. From Model (9), we have

$$\begin{aligned} H_{n+1} &\leq (\rho_1 H_n) \\ P_{n+1} &\leq (\rho_2 H_n) \\ G_{n+1} &\leq \alpha_0 G_n + \alpha H_n + (1-\alpha) P_n. \end{aligned}$$

By the assumptions, we conclude

$$\begin{aligned} \lim_{n\to\infty} \sup(H_n) &\leq (\rho_1 H_n) \leq \rho_1 \\ \lim_{n\to\infty} \sup(P_n) &\leq (\rho_2 H_n) \leq \rho_1 \\ \lim_{n\to\infty} \sup(G_n) &\leq \frac{\rho_1}{1-\alpha_0}. \end{aligned}$$

Hence, we have

$$\lim_{n\to\infty} \sup(H_n, P_n, G_n) \leq \frac{\rho_1}{1-\alpha_0}.$$

Moreover, a conclusion implies that

$$\lim_{n\to\infty} \inf(H_n, P_n, G_n) \geq 1.$$

Consuming $\mu_1 = 1$ and $\mu_2 = \dfrac{\rho_1}{1-\alpha_0}$ which leads that Model (9) is a permanent system achieving

$$1 \leq \lim_{n\to\infty} \inf(H_n, P_n, G_n) \leq \lim_{n\to\infty} \sup(G_n) \leq \frac{\rho_1}{1-\alpha_0}.$$

Continue the second part, as follows:

$$\begin{aligned}
&\sup_{u\in U}\inf_{v\in V} G(H,P) \le \inf_{v\in V}\sup_{u\in U} G(H,P)\\
&\Rightarrow \sup_{u\in U}(1) \le \inf_{v\in V}\left(\frac{\rho_1}{1-\alpha_0}\right)\\
&\Rightarrow 1 \le \frac{1}{1-\alpha_0},
\end{aligned}$$

where $U = V = \mathbb{R}_+$. Thus, the model has a saddle surface. □

Remark 1. *Model* (9) *satisfies the chaos in the third equation for* $\alpha_0 \to 0$ *such that*

$$\begin{aligned}
H_{n+1} &= (\rho_1 H_n)\,(\tanh(P_n))\\
P_{n+1} &= (\rho_2 H_n)\,(1-\tanh(P_n))\\
G_{n+1} &= \alpha H_n + (1-\alpha)P_n.
\end{aligned} \tag{13}$$

And when $\alpha_0 \to 1$, *we get the chaos difference system*

$$\begin{aligned}
\eth(H_n) &= (\rho_1 H_n)\,(\tanh(P_n)) - H_n\\
\eth(P_n) &= (\rho_2 H_n)\,(1-\tanh(P_n)) - P_n\\
\eth(G_n) &= \alpha H_n + (1-\alpha)P_n,
\end{aligned} \tag{14}$$

corresponding to the linear model

$$\begin{aligned}
\eth(H_n) &= -H_n\\
\eth(P_n) &= -P_n\\
\eth(G_n) &= \alpha H_n + (1-\alpha)P_n,
\end{aligned} \tag{15}$$

and to the optimal model, when $\tanh(P) \approx 1$

$$\begin{aligned}
\eth(H_n) &= (\rho_1 - 1)H_n\\
\eth(P_n) &= -P_n\\
\eth(G_n) &= \alpha H_n + (1-\alpha)P_n,
\end{aligned} \tag{16}$$

3.1. Chaos control of model (11)

Model (11) can be controlled by 2D-controller law as follows:

$$U_H = -\,(\rho_1 H)\,(\tanh(P_n)) \tag{17}$$

$$U_P = -\,(\rho_2 H)\,(1-\tanh(P_n))\,. \tag{18}$$

The third equation can be controlled by suggesting values of α and $\alpha_0 \in (0,1)$. Figures 6 and 7 showed that the optimal interval for $\alpha_0 \in (0, 0.5)$ and $\alpha \in (0, 0.4)$.
We have the following result

Theorem 2. *The Model* (11) *can be controlled by 2D-controller* (17).

Proof. The controlled model can be recognized as follows:

$$\begin{aligned} \eth(H) &= (\rho_1 H)\,(\tanh(P)) - H - U_H \\ \eth(P) &= (\rho_2 H)\,(1 - \tanh(P)) - P - U_P \\ \eth(G) &= \alpha H + (1-\alpha)P - (1-\alpha_0)G. \end{aligned} \tag{19}$$

□

Substituting (17) in (19), we obtain

$$\begin{aligned} \eth(H) &= -H \\ \eth(P) &= -P \\ \eth(G) &= \alpha H + (1-\alpha)P - (1-\alpha_0)G. \end{aligned} \tag{20}$$

In matrix form, we have

$$\begin{pmatrix} \eth(H) \\ \eth(P) \\ \eth(G) \end{pmatrix} = \begin{pmatrix} -1 & 0 & 0 \\ 0 & -1 & 0 \\ \alpha & (1-\alpha) & -(1-\alpha_0) \end{pmatrix} \begin{pmatrix} H \\ P \\ G \end{pmatrix}. \tag{21}$$

The goal is to prove that the zero equilibrium of (20) is asymptotically stable, which indicates that the model states converge towards zero as time progresses. Since all the eigenvalues $\lambda_{1,2} = -1, \lambda_3 = -(1-\alpha_0), \alpha_0 \in (0,1)$ of the model are negative; then by the stability theorem, we have that the zero outcomes is asymptotically stable and, thus the system is stabilized.

3.2. Discrete Lyapunov formula (DLF)

The DLF is given by the structure

$$\Sigma\chi\Sigma^c - \chi + \Theta = 0$$

where Θ is a Hermitian matrix and Σ^c is the conjugate transpose of Σ. It is well known that for $\Theta > 0$ there exists a unique $\Delta > 0$ such that $\Sigma^\top \Delta \Sigma - \Delta + \Theta = 0$ if and only if the model is asymptotically stable. In view of Theorem 2, the Model (11) is asymptotically stable for $\alpha \in (0,1), \alpha_0 \in (0,1)$, which leads to satisfy the DLF, where $\chi^\top \Delta \chi$ is the Lyapunov formula. Next example shows the DLF for Model (21) with different parameters (see Figure 8).

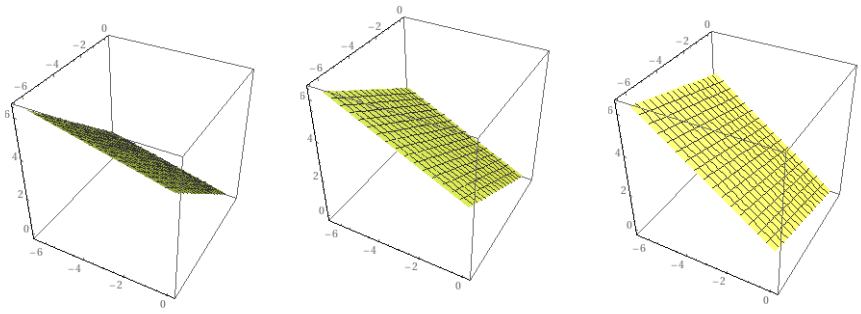

Figure 8. The 3D-plot of the linear Model (21), when $\alpha = 0.25, 0.5, 0.75, \alpha_0 \approx 1$ respectively.

Example 1. *Let the following data hold*

- $\alpha = 0.25, \alpha_0 = 0.75$ *then DLF is*

$$\left[\begin{pmatrix} -1 & 0 & 0 \\ 0 & -1 & 0 \\ 0.25 & 0.75 & -0.25 \end{pmatrix}, \begin{pmatrix} -0.0608116 & -0.002466 & -0.0243887 \\ -0.002466 & -0.0001 & -0.000989 \\ -0.0243887 & -0.000989 & -0.00978121 \end{pmatrix}\right],$$

  where the solution is $\begin{pmatrix} 0.2466 \\ 0.01 \\ 0.0989 \end{pmatrix}$;

- $\alpha = \alpha_0 = 0.5$ *the DLF is given by*

$$\left[\begin{pmatrix} -1 & 0 & 0 \\ 0 & -1 & 0 \\ 0.5 & 0.5 & -0.5 \end{pmatrix}, \begin{pmatrix} -0.36 & -0.03 & -0.0006 \\ -0.03 & -0.0025 & -0.00005 \\ -0.0006 & -0.00005 & -1 \times 10^{-6} \end{pmatrix}\right],$$

  for the solution $\begin{pmatrix} 0.6 \\ 0.05 \\ 0.001 \end{pmatrix}$.

- $\alpha = 0.75, \alpha_0 = 0.25$, *then*

$$\left[\begin{pmatrix} -1 & 0 & 0 \\ 0 & -1 & 0 \\ 0.75 & 0.25 & -0.5 \end{pmatrix}, \begin{pmatrix} -0.81 & -0.135 & -0.009 \\ -0.135 & -0.0225 & -0.0015 \\ -0.009 & -0.0015 & -0.0001 \end{pmatrix}\right]$$

  where the solution is $\begin{pmatrix} 0.9 \\ 0.15 \\ 0.01 \end{pmatrix}$;

- $\alpha = 0.75, \alpha_0 = 0.25$ *then*

$$\left[\begin{pmatrix} -1 & 0 & 0 \\ 0 & -1 & 0 \\ 0.75 & 0.25 & -0.75 \end{pmatrix}, \begin{pmatrix} -1. & -0.25 & -0.02 \\ -0.25 & -0.0625 & -0.005 \\ -0.02 & -0.005 & -0.0004 \end{pmatrix}\right]$$

with the solution $\begin{pmatrix} 1 \\ 0.25 \\ 0.02 \end{pmatrix}$;

- $\alpha = 0.75, \alpha_0 = 0$ *then, we get*

$$\left[\begin{pmatrix} -1 & 0 & 0 \\ 0 & -1 & 0 \\ 0.75 & 0.25 & -1 \end{pmatrix}, \begin{pmatrix} -1. & -0.25 & -0.02 \\ -0.25 & -0.0625 & -0.005 \\ -0.02 & -0.005 & -0.0004 \end{pmatrix}\right]$$

satisfying the solution $\begin{pmatrix} 1 \\ 0.25 \\ 0.021 \end{pmatrix}$.

- $\alpha = 0.34, \alpha_0 = 0.45$, *then DLF is*

$$\left[\begin{pmatrix} -1 & 0 & 0 \\ 0 & -1 & 0 \\ 0.34 & 0.6 & -0.6 \end{pmatrix}, \begin{pmatrix} -4. & -2.5 & -0.4 \\ -2.5 & -1.5625 & -0.25 \\ -0.4 & -0.25 & -0.04 \end{pmatrix}\right]$$

having the outcome $\begin{pmatrix} 2 \\ 1.25 \\ 0.2 \end{pmatrix}$.

Note that, the last solution is controlled by the hosted and decreases the parasitiod providing $\rho_1 = \rho_2$ (see Figure 9).

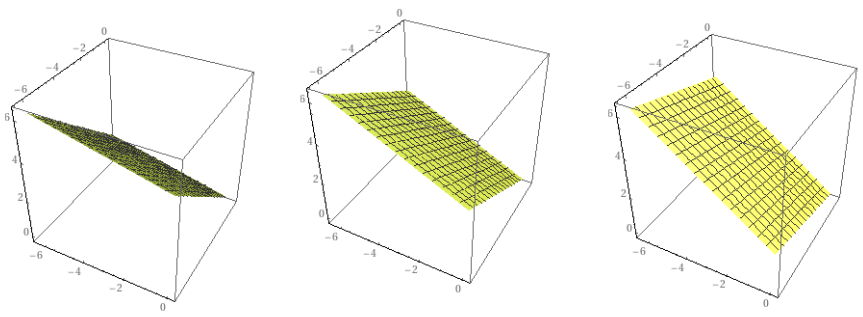

Figure 9. The 3D-plot of the linear Model (21), when $\alpha = 0.25, 0.5, 0.75, \alpha_0 \approx 1$ respectively.

4. Discussions

The Model (21) achieves

$$Rank\begin{pmatrix} -1 & 0 & 0 \\ 0 & -1 & 0 \\ \alpha & (1-\alpha) & -(1-\alpha_0) \end{pmatrix} = 3$$

and all the matrices in the above example satisfy $Rank < 3$. The low-rank DLFs is of pronounced significance, where normally hard to calculate in control system investigation and strategy. Opportunely, Mesbahi and Papavassilopoulos [19] presented that under some conditions, the lowest-rank results of the DLF can be professionally solved by linear programming.

In [20], the authors proved that the lowest-rank results of both the continuous and discrete Lyapunov formulas over symmetric shape (like tanh function) are unique and can be precisely resolved by their convex relaxations and the symmetric linear programming issues. Proposition 4.4 in [20] indicated that the unique outcome could select an exact lowest-rank solution to DLF over the symmetric shape to its trace minimization relaxation issue. Therefore, all solutions in Example 1 are unique for a set of parameters.

5. Conclusions

A 3D-mathematical model for the Vector-Borne Disease is formulated. The design assumes three sub-populations: the human population (H), the vector population (P) and the parasitic transmission media (G). The design equilibrium explanations were indicated, and the environments for their stability were recognized. A numerical solution to the model was recognized utilizing the discrete Lyapunov formulas were simulated for different values of parameters of the disease situation, Figures 5–8. Our simulations show that control actions, which minimize the population rank, the human-vector transmission rate as well as vector-human transmission media (such as garbage collection and removal, dirty food, body-liquids or substances, by airborne breath). Hence, control processes that address these fixed factorize (disease transmission parameters) would be valuable in the attempt towards the annihilation of the infection.

Conflict of interest

The author declares that there is no competing interests.

References

1. Mattingly, P. Frederick, The biology of mosquito-borne disease, The biology of mosquito-borne disease, 1969. doi: 10.1136/bmj.1.5647.835.
2. C. Dye, Models for the population dynamics of the yellow fever mosquito, Aedes aegypti, *J. Anim. Ecol.*, **53** (1984), 247–268. doi: 10.2307/4355.
3. R. M. May, Biological populations with non overlapping generations: stable points, stable cycles, and chaos, *Science*, **186** (1974), 645–647. doi: 10.1126/science.186.4164.645.
4. T. S. Bellows, The descriptive properties of some models for density dependence, *J. Anim. Ecol.*, **50** (1981), 139–156. doi: 10.2307/4037.
5. X. Ma, Q. Din, M. Rafaqat, N. Javaid, Y. Feng, A density-dependent host-parasitoid model with stability, bifurcation and chaos control, *Mathematics*, **8** (2020), 536. doi: 10.3390/math8040536.
6. H. A. Jalab, R. W. Ibrahim, New activation functions for complex-valued neural network, *Int. J. Phys. Sci.*, **6** (2011), 1766–1772.

7. R. W. Ibrahim, Utility function for intelligent access web selection using the normalized fuzzy fractional entropy, *Soft Comput.*, (2020), 1–8.
8. Q. Din, Global behavior of a host-parasitoid model under the constant refuge effect, *Appl. Math. Model.*, **40** (2016), 2815–2826. doi: 10.1016/j.apm.2015.09.012.
9. S. M. Sajjad, Q. Din, M. Safeer, M. Asif Khan, K. Ahmad, A dynamically consistent nonstandard finite difference scheme for a predator-prey model, *Adv. Differ. Equ-NY,* **1** (2019), 1–17. doi: 10.1186/s13662-019-2319-6.
10. Q. Din, K. Haider, Discretization, bifurcation analysis and chaos control for Schnakenberg model, *J. Math. Chem.*, **58** (2020), 1615–1649. doi: 10.1007/s10910-020-01154-x.
11. M. Islam, Mathematical Modeling of the Garbage Collection Problem, *Math. Model. Appl. Comput.*, **4** (2013), 29–38.
12. H. Natiq, N. M. G. Al-Saidi, M. R. M. Said, A. Kilicman, A new hyperchaotic map and its application for image encryption, *Eur. phys. J. Plus*, **133** (2018), 1–14. doi: 10.1140/epjp/i2018-11834-2.
13. N. M. G. Al-Saidi, D. Younus, H. Natiq, M. R. K. Ariffin, Z. Mahad, A New hyperchaotic map for a secure communication scheme with an experimental realization, *Symmetry*, **12** (2020), 1881. doi: 10.3390/sym12111881.
14. A. K. Farhan, N. M. G. Al-Saidi, A. T. Maolood, F. Nazarimehr, I. Hussain, Entropy analysis and image encryption application based on a new chaotic system crossing a cylinder, *Entropy*, **21** (2019), 958. doi: 10.3390/e21100958.
15. M. S. Fadhil, A. K. Farhan, M. N. Fadhil, N. M. G. Al-Saidi, A New Lightweight AES Using a Combination of Chaotic Systems, *2020 IEEE first conference on information Technology to Enhance E-learning and Other Applications (IT-ELA)*, (2020), 82–88.
16. P. S. Sadeghi, Z. Rostami, V. Pham, F. E. Alsaadi, T. Hayat, Modeling of neurodegenerative diseases using discrete chaotic systems, *Commun. Theor. Phys.*, **71** (2019), 1241. doi: 10.1088/0253-6102/71/10/1241.
17. R. W. Ibrahim, D. Altulea, Controlled homeodynamic concept using a conformable calculus in artificial biological systems, *Chaos, Solitons Fract.*, **140** (2020), 110–132. doi: 10.1016/j.chaos.2020.110132.
18. L. Stephen, Dynamical Systems with Applications Using Mathematica, *Boston: Birkhauser*, 2007.
19. M. Mesbahi, G. P. Papavassilopoulos. On the rank minimization problem over a positive semidefinite linear matrix inequality, *IEEE T. Automat. Contr.*, **42** (1997), 239–243. doi: 10.1109/9.554402.
20. Z. Luo, J. Tao, N. Xiu, Lowest-rank solutions of continuous and discrete Lyapunov equations over symmetric cone, *Linear Algebra Appl.*, **452** (2014), 68–88. doi: 10.1016/j.laa.2014.03.028.

AIMS Press